CHAPTER 3

METHODOLOGY AND NUMERICAL SIMULATION

3.1 INTRODUCTION

In this chapter, the computational methods used to simulate the nitrogen gas discharge are discussed. The details of the numerical simulation are also emphasized. Some important equations such as the Poisson's equation, circuit equation and Sato's equation are explained in detail. The Phoenical LPE SHASTA is the version of the FCT adopted in this study.

3.2 CIRCUIT EQUATIONS

The C-to-C electrical discharge can be modeled as the LCR circuit shown as Fig(3.2.1). The circuit characteristics and its oscillation behavior can be mathematically represented by four major equations as written below:

$$\frac{dI_1}{dt} = -\frac{R_1}{L_1} I_1 + \frac{1}{L_1} V_1 - \frac{1}{L_1} V_2$$

$$\frac{dI_2}{dt} = \frac{1}{L_2} V_2 - \frac{1}{L_2} I_2 R_{eff}$$

$$\frac{dV_1}{dt} = -\frac{1}{C_1} I_1$$

$$\frac{dV_2}{dt} = \frac{1}{C_2}(I_1 - I_2) \qquad 3.2.1$$

where the effective resistance, R_{eff} is determined by

$$R_{eff} = \frac{R_{gap} R_{bypass}}{R_{gap} + R_{bypass}} \qquad 3.2.1a$$

The bypass resistor, R_{bypass} is initially set as 5kΩ, and the gap resistance is determined by the equation below

$$R_{gap} = \frac{V_2}{i}, \qquad 3.2.1b$$

where i is the internal current in the gap due to the motion of the charge particles. This current will be determined by Sato's equation. The more detailed discussions on Sato's equation will be carried out at section 3.8 in this chapter.

These equations are written as ordinary first order differential equations. Numerically solution of these equations is carried out using the fourth order Runge-Kutta method (RK-4).

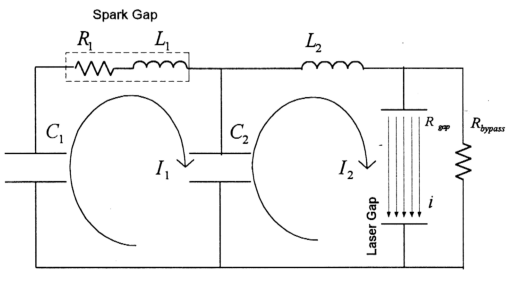

Figure 3.2.1: Capacitor Transfer Circuit Or C-To-C Discharge Circuit

3.2.1 FOURTH-ORDER RUNGE-KUTTA METHOD (RK-4)

Let us consider an ordinary differential equation

$$\frac{dY}{dt} = f(Y, x) \qquad 3.2.2$$

The basic idea of the fourth-order Runge-Kutta method (RK-4) is evaluating this function, f, at four selected points and use slope estimates k_1, k_2, k_3 and k_4 whose weighted average is ΔY_j. In particular, the setting is shown as below:

$$k_1 = hf(x_j, Y_j)$$

$$k_2 = hf\left(x_j + \frac{h}{2}, Y_j + \frac{k_1}{2}\right)$$

$$k_3 = hf\left(x_j + \frac{h}{2}, Y_j + \frac{k_2}{2}\right)$$

$$k_4 = hf(x_j + h, Y_j + k_3) \qquad 3.2.3$$

where h is the step size for x.

In summary, the solution of this function, f is

$$Y_{j+1} = Y_j + \frac{k_1 + 2k_2 + 2k_3 + k_4}{6} \qquad 3.2.4$$

3.2.2 NUMERICAL SOLUTION OF THE CIRCUIT EQUATIONS

The four circuit equations Eq(3.2.3) can be easily solved by using the RK-4 method. These values of I_1, I_2, V_1 and V_2 for the next time step are calculated. The gap voltage, V_{gap}, can be easily determined by the Ohm's law, $V_{gap} = I_2 R_{eff}$.

The different symbols of k, l, m and n are used corresponding to the values of V_1, V_2, I_1 and I_2. The numerical solutions are listed as below:

$$k_1 = \Delta t * \left(-\frac{1}{C_1}(I_1) \right)$$

$$l_1 = \Delta t * \left(\frac{1}{C_2}(I_1 - I_2) \right)$$

$$m_1 = \Delta t * \left(-\frac{R_1}{L_1}(I_1) + \frac{1}{L_1}(V_1) - \frac{1}{L_1}(V_2) \right)$$

$$n_1 = \Delta t * \left(\frac{1}{L_2}(V_2) - \frac{1}{L_2}(I_2 R_{eff}) \right) \qquad 3.2.5$$

and the following steps are:

$$k_2 = \Delta t * \left(-\frac{1}{C_1}(I_1 + 0.5 * m_1) \right)$$

$$l_2 = \Delta t * \left(\frac{1}{C_2}((I_1 + 0.5 * m_1) - (I_2 + 0.5 * n_1)) \right)$$

$$m_2 = \Delta t * \left(-\frac{R_1}{L_1}(I_1 + 0.5 * m_1) + \frac{1}{L_1}(V_1 + 0.5 * k_1) - \frac{1}{L_1}(V_2 + 0.5 * l_1) \right)$$

$$n_2 = \Delta t * \left(\frac{1}{L_2}(V_2 + 0.5 * l_1) - \frac{1}{L_2}(I_2 + 0.5 * n_1) R_{eff} \right) \qquad 3.2.6$$

and

$$k_3 = \Delta t * \left(-\frac{1}{C_1}(I_1 + 0.5 * m_2) \right)$$

$$l_3 = \Delta t * \left(\frac{1}{C_2}((I_1 + 0.5 * m_2) - (I_2 + 0.5 * n_2)) \right)$$

$$m_3 = \Delta t * \left(-\frac{R_1}{L_1}(I_1 + 0.5 * m_2) + \frac{1}{L_1}(V_1 + 0.5 * k_2) - \frac{1}{L_1}(V_2 + 0.5 * l_2) \right)$$

$$n_3 = \Delta t * \left(\frac{1}{L_2}(V_2 + 0.5 * l_2) - \frac{1}{L_2}(I_2 + 0.5 * n_2) R_{eff} \right) \qquad 3.2.7$$

and

$$k_4 = \Delta t * \left(-\frac{1}{C_1}(I_1 + m_3) \right)$$

$$l_4 = \Delta t * \left(\frac{1}{C_2}((I_1 + m_3) - (I_2 + n_3)) \right)$$

$$m_4 = \Delta t * \left(-\frac{R_1}{L_1}(I_1 + m_3) + \frac{1}{L_1}(V_1 + k_3) - \frac{1}{L_1}(V_2 + l_3) \right)$$

$$n_4 = \Delta t * \left(\frac{1}{L_2}(V_2 + l_3) - \frac{1}{L_2}(I_2 + n_3)R_{eff} \right) \qquad 3.2.8$$

Finally, the new values at the new time $t' = t + \Delta t$ can be calculated as below,

$$V_1' = V_1 + \frac{k_1 + 2k_2 + 2k_3 + k_4}{6}$$

$$V_2' = V_2 + \frac{l_1 + 2l_2 + 2l_3 + l_4}{6}$$

$$I_1' = I_1 + \frac{m_1 + 2m_2 + 2m_3 + m_4}{6}$$

$$I_2' = I_2 + \frac{n_1 + 2n_2 + 2n_3 + n_4}{6} \qquad 3.2.9$$

The value of the gap voltage, V_{gap} can be directly determined with equation

$$V_{gap} = I_2' R_{eff} \qquad 3.2.10$$

The voltage of the gap, V_{gap} is important in calculating the electrical field of the discharge channel which will be discussed at the next section.

3.3 THE STUDY OF THE ELECTRICAL FIELD

In this study, the simulation of the electrical field of the discharge gap have been carried out in both ways, there are the uniform distribution electrical field and the non-uniform electrical field.

3.3.1 UNIFORM ELECTRICAL FIELD

Under the uniform distribution of the electrical field, some important assumptions had been made. Firstly, the charged densities are distributed uniformly in the discharge gap and the current fluxes are consistent all along the mesh. Secondly, the electrodes are perfect absorbing and emitting materials.

The value of the electrical field can easily be calculated by using the equation as below:

$$E(t) = \frac{V_{gap}(t)}{d} \qquad 3.3.1$$

where d is the distance between the discharge electrodes.

3.3.2 NON-UNIFORM ELECTRICAL FIELD

The non-uniform electrical field is caused by the space charge effect inside the discharge gap.

The motion of the electrons is very large when compared to the motion of the ions. Therefore, the value of the electron flux is larger than the ion flux. This will cause space charge effects and cathode sheath is formed, since the cathode is not a perfect emitting material. The electrons will be released from the cathode under the secondary Townsend emission, where the positive ion bombardment plays a significant role to free the electrons after the collision process under the high electrical field. In this case, there is always a net

charge density in the discharge gap and the electrical field is not uniform as discussed in the previous section.

3.3.3 POISSON EQUATION

In order to calculate the non-uniform electrical field distribution, we need to calculate the total net charge densities at the particular mesh. The distribution for space and time variation can be determined by using the Poisson equation as below:

$$\nabla \cdot E(x,t) = -\frac{e}{\varepsilon_o}\left(n_i(x,t) - n_e(x,t)\right) \qquad 3.3.2$$

where e is the electron charge and ε_o is the permittivity of free space.

3.4 LOCAL ELECTRICAL FIELD BETWEEN THE ELONGATED PARALLEL PLATES

The gap geometry plays an important role while simulating the electrical field. These plates' dimension, where the electrode length is always larger then the electrode separation, imposes the choice of the appropriate model used to calculate the space charge field.

The assumption is made that the electron and ion population are distributed uniformly in parallel planes with a surface charge density, σ C/cm^2.

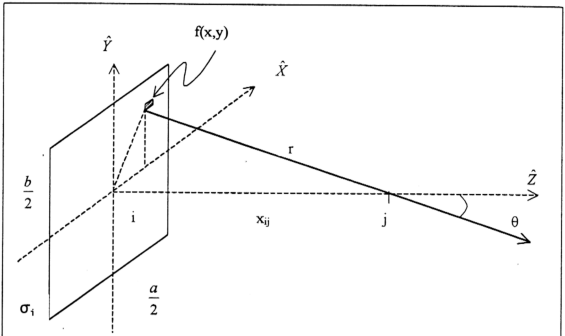

Figure 3.4.1:Parallel Planes Charge Simulation Used For Electrical Field Calculation

Fig(3.4.1), we can identify the local electrical field at any point, j, which is affected by a surface charge, and represented by a partial differential equation as below:

$$\delta E = \frac{\sigma_i \delta x \delta y}{4\pi\varepsilon_o r^2} \cos\theta \qquad 3.4.1$$

where $\delta x \delta y$ leads to a surface integral.

From the geometrical diagram, we can determine

$$\cos\theta = \frac{x_{ij}}{\left(x^2 + y^2 + x_{ij}^2\right)^{1/2}}, \qquad 3.4.2a$$

and

$$r^2 = \left(x^2 + y^2 + x_{ij}^2\right) \qquad 3.4.2b$$

where $i, j = 1,2,\ldots,n$

Point i is the location of the surface charge while j is the point where the local electrical field is calculated. x_{ij} is the distance between point i and j

After substituting Eq(3.4.2a) and Eq(3.4.2b) into Eq(3.4.1), we can get

$$\delta E = \frac{\sigma_i x_{ij}}{4\pi\varepsilon_o} \frac{\delta x \delta y}{\left(x^{2+} y^2 + x_{ij}^2\right)^{3/2}} \qquad 3.4.3$$

Consider the integration from $0 \le x \le a/2$ and $0 \le y \le b/2$, Eq(3.4.3) will become

$$E(j) = \frac{1}{4\pi\varepsilon_o} \int_0^{b/2} \int_0^{a/2} \frac{\sigma_i x_{ij}}{\left(x^{2+} y^2 + x_{ij}^2\right)^{3/2}} dxdy \qquad 3.4.4$$

While calculating the total planar area, we can have

$$E(j) = \frac{1}{\pi\varepsilon_o} \int_0^{b/2} \int_0^{a/2} \frac{\sigma_i x_{ij}}{\left(x^{2+} y^2 + x_{ij}^2\right)^{3/2}} dxdy \qquad 3.4.5$$

From the Eq(3.4.5), we can solve the integration readily,

$$\int_0^{b/2} \int_0^{a/2} \frac{\sigma_i x_{ij}}{\left(x^2 + y^2 + x_{ij}^2\right)^{3/2}} dxdy = \int_0^{b/2} \frac{x}{\left(x^2 + x_{ij}^2\right)\left(x^{2+} y^2 + x_{ij}^2\right)^{1/2}} \Big|_{x=0}^{a/2} dy$$

$$= \frac{1}{x_{ij}} arctg \frac{xy}{x_{ij}\left(x^2 + y^2 + x_{ij}^2\right)^{1/2}} \Big|_{x=0}^{a/2} \Big|_{y=0}^{b/2}$$

3.4.6

Finally, the local electrical field, $E(j)$ at point, j, which is affected by a surface charge can be simplified into

$$E(j) = \frac{\sigma_i}{\pi x_{ij}} arctg \frac{xy}{x_{ij}\left(x^2 + y^2 + x_{ij}^2\right)^{1/2}} \Big|_{x=0}^{a/2} \Big|_{y=0}^{b/2} \qquad 3.4.7$$

3.4.1 SIMULATION OF THE ELECTRICAL FIELD VARIATION

The total effect of the local electrical field $E(j)$ at point j can be calculated by summation of all the surface charge.

$$E(j) = \sum_{i}^{n} \frac{\sigma_i}{\pi x_{ij}} arctg \frac{xy}{x_{ij}\left(x^2 + y^2 + x_{ij}^2\right)^{1/2}} \Bigg|_{x=0}^{y/2} \Bigg|_{y=0}^{y/2} \qquad 3.4.8$$

where $i = 1,2,...,n$ and $i \neq j$

$$E(j) = \sum_{i}^{n} \frac{\sigma_i}{2\pi x_{ij}} arctg \frac{ab}{x_{ij}\left(a^2 + b^2 + 4x_{ij}^2\right)^{1/2}} \qquad 3.4.9$$

Calculation can be done for the series j and a series of local electrical field variation $E(x,t)$ at the particular time t can be determined.

Besides the local electrical field, electrons and ions in the discharge channel will also experience the external static electrical field. The total electrical field is actually a combination of both the external static and local electrical fields.

3.5 PHOENICAL LPE SHASTA FLUX CORRECTED TRANSPORT

In this study, the Phoenical LPE SHASTA Flux-Corrected Transport as a version of the FCT algorithms is used. This version of the FCT algorithm had been tested by Boris and Book on its stability and accuracy (Boris and Book, 1976; Morrow, 1981).

3.5.1 DIFFUSION COEFFICIENTS AND LOW PHASE ERRORS

From the previous discussion, we know that we need to carefully select the diffusion coefficients, $\nu_{i\pm\frac{1}{2}}$ as we simulate the fluid behavior of the plasma. There are many alternatives of choosing the diffusion coefficients, $\nu_{i\pm\frac{1}{2}}$ depending on the versions and types of FCT algorithms. From the previous investigation done by Book and Boris (1976a,

1976b), there are some versions of FCT algorithms that had been studied and tested for their efficiencies.

One of the most common versions of the FCT algorithms is the Phoenical LPE SHASTA FCT algorithm. This SHASTA (Sharp And Smooth Transport Algorithm) has been tested by Book and Boris (1973, 1976a, 1976b) and show positive results as a Low Phase Error (LPE) algorithm.

In this version of FCT algorithm, the diffusion coefficients, $\nu_{i\pm\frac{1}{2}}$ are chosen as below

$$\nu_{i\pm\frac{1}{2}} = \frac{1}{6} + \frac{1}{3}\varepsilon^2_{i+\frac{1}{2}} \qquad 3.5.1$$

The result shows that Phoenical LPE SHASTA FCT algorithm has a small absolute error. This is comparable with the other algorithms, such as Lax-Wendroff or Leapfrog methods. The new version of FCT algorithm is 3-4 times better in taking care of numerical errors as compared with these methods.

3.5.2 NUMERICAL SOLUTION OF PHOENICAL LPE SHASTA FLUX CORRECTED TRANSPORT

The Phoenical LPE SHASTA version of flux corrected transport takes the following steps:

a. Compute a transported and diffused solution of provisional value, $\tilde{\rho}_i$, using an equation

$$\tilde{\rho}_i = \rho_i^o - \frac{1}{2}\left(\varepsilon_{i+\frac{1}{2}}\left(\rho^o_{i+1} + \rho^o_i\right) - \varepsilon_{i-\frac{1}{2}}\left(\rho_i^o + \rho^o_{i-1}\right)\right) + \left(\upsilon_{i+\frac{1}{2}}\left(\rho^o_{i+1} + \rho^o_i\right) - \upsilon_{i-\frac{1}{2}}\left(\rho_i^o + \rho^o_{i-1}\right)\right)$$

3.5.2

where $\varepsilon_{i\pm\frac{1}{2}} = \upsilon_{i\pm\frac{1}{2}} \frac{\Delta t}{\Delta x}$ and $\upsilon_{i\pm\frac{1}{2}}$ is the flow velocity half way between grid points i and $i+1$ calculated in this case by simple averaging. The diffusion coefficients as a version of Phoenical LPE SHASTA, are written as below:

$$\nu_{i\pm\frac{1}{2}} = \frac{1}{6} + \frac{1}{3}\varepsilon^2_{i+\frac{1}{2}} \qquad 3.5.3$$

b. Compute the raw antidiffusive fluxes, $f^{ad}_{i\pm\frac{1}{2}}$, which in our cas for the Phoenical version are

$$f^{ad}_{i+\frac{1}{2}} \equiv \mu_{i+\frac{1}{2}}\left(\widetilde{\rho}_{i+1} - \widetilde{\rho}_i + \left(-\rho^o_{i+2} + 3\rho^o_{i+1} - 3\rho^o_i + \rho^o_{i-1}\right)/6\right) \qquad 3.5.4$$

where $\mu_{i+\frac{1}{2}} = \frac{1}{6} - \frac{1}{6}\varepsilon^2_{i+\frac{1}{2}}$ 3.5.5

c. Compute corrected antidiffusive fluxes, $f^c_{i\pm\frac{1}{2}}$, using

$$f^c_{i+\frac{1}{2}} \equiv S \cdot \max\left\{0, \min\left[S\cdot(\widetilde{\rho}_{i+2} - \widetilde{\rho}_{i+1}), \left|f^{ad}_{i+\frac{1}{2}}\right|, S\cdot(\widetilde{\rho}_i - \widetilde{\rho}_{i-1})\right]\right\} \qquad 3.5.6$$

where $|S| = 1$ and sign $S \equiv sign(\widetilde{\rho}_{i+2} - \widetilde{\rho}_{i+1})$.

d. Perform antidiffusion using

$$\rho^n_i = \widetilde{\rho}_i - f^c_{i+\frac{1}{2}} + f^c_{i-\frac{1}{2}} \qquad 3.5.7$$

Thus ρ^n_i is the required solution at $t + \Delta t$.

3.6 TOWNSEND IONIZATION PROCESS IN THE DISCHARGE MEDIUM

When the discharge is taking place in the laser channel between the two electrodes, the charged carriers will be accelerated and traveled along the discharge medium. These carriers will experience the creation of new pairs of charges of electrons and ions. This incident is due to the ionization process in the discharge medium as explained by Townsend

(1910). At the same time, the number of the carriers would be reduced due to the loss of electrons and ions during the recombination and attachment processes.

3.6.1 FLUID EQUATIONS WITH SOURCE TERM

In order to model the Townsend process in a gaseous discharge, the fluid equation at Eq(2.6.1*b*) can be rewritten by now adding a source term, S. This equation in 1-dimesional forms shown as below:

$$\frac{\partial \rho}{\partial t} = S - \frac{\partial \rho \upsilon}{\partial x} \qquad 3.6.1$$

where t is the time variable; x is the space variable; ρ is the charged carrier number densities and υ is the drift velocity of the charged carriers.

If writing in terms of electron and ion densities n_i and n_e respectively, the equation will take the following form:

$$\frac{\partial n_e}{\partial t} + \frac{\partial n_e u_e}{\partial x} = S(n_e)$$

$$= n_e |u_e| \alpha\left(\frac{E}{P}(x,t)\right) - n_e n_i \beta\left(\frac{E}{P}(x,t)\right) \qquad 3.6.2a$$

$$\frac{\partial n_i}{\partial t} + \frac{\partial n_i u_i}{\partial x} = S(n_e)$$

$$= n_e |u_e| \alpha\left(\frac{E}{P}(x,t)\right) - n_e n_i \beta\left(\frac{E}{P}(x,t)\right) \qquad 3.6.2b$$

where u_e and u_i are electron and ion mean velocities, α and β are the first ionization and radiative recombination coefficients respectively.

3.6.2 NUMERICAL SOLUTION OF THE SOURCE TERM IN THE FLUID EQUATION

For the simple Euler method of solution, the source terms can be simply added to the convective term. Hence,

$$\Delta\rho = \Delta t\left(S_i^n - \frac{\partial \rho_i^n \upsilon_i^n}{\partial x}\right)$$

$$= \Delta t\left(S_i^n\right) - \Delta\rho_c \qquad 3.6.3$$

However, this solution is not suitable to be used specially in the FCT codes (Morrow, 1981). A higher order numerical solution is needed, as for the convective term, $\Delta\rho_c$, since the FCT treats it with higher order of accuracy. For this purpose, an auxiliary step was introduced.

In this auxiliary step, the complete $\Delta\rho_{T_{1/2}}$ at half the time step is calculated by using the equation

$$\Delta\rho_{T_{1/2}} = \frac{\Delta t}{2}\left(S_i^n\right) + \frac{\Delta\rho_c}{2} \qquad 3.6.4$$

This important step allows the auxiliary values for the source terms, $S_i^{n+\frac{1}{2}}$ to be calculated, as shown in the Eq(3.6.2). Then a full step was calculated, using the equation

$$\Delta\rho_T = \Delta t\left(S_i^{n+\frac{1}{2}}\right) + \Delta\rho_c \qquad 3.6.5$$

While comparing the Eq(3.6.3) and Eq(3.6.5), the auxiliary values for the source terms, $S_i^{n+\frac{1}{2}}$ is the better choice when compared to the S_i^n.

The order of accuracy can be increased further if the double auxiliary step is taken. The quarter time step of convective term, $\Delta\rho_{T_{1/4}}$ is calculated and the correspondence source terms, $S_i^{n+\frac{1}{4}}$ can be determined. The numerical solutions are as below:

$$\Delta\rho_{\tau_{1/4}} = \frac{\Delta t}{4}\left(S_i^n\right) + \frac{\Delta\rho_c}{4} \qquad 3.6.6$$

together with

$$\Delta\rho_{\tau_{1/2}} = \frac{\Delta t}{2}\left(S_i^{n+\frac{1}{4}}\right) + \frac{\Delta\rho_c}{2} \qquad 3.6.7$$

and

$$\Delta\rho_T = \Delta t\left(S_i^{n+\frac{1}{2}}\right) + \Delta\rho_c \qquad 3.6.8$$

The accuracy of the single auxiliary step and double auxiliary step will be tested and investigated in this study.

3.6.3 BOUNDARY CONDITION OF THE FLUID EQUATION

In a gas discharge, the velocity of the ion is so small when compared to the electron. This leads to the formation of the space charge.

Since the main purpose of this study is focused on the space charge effects and the sheath formation at the cathode, the anode sheath formation is assumed to be very small and negligible. We can assume that the anode is a perfectly absorbing and emitting material. The electron and ion fluxes are always consistent at the anode. It is assumed that there is no space charge formed at the anode.

However, the cathode can emit electrons if there is enough energy for the ions on bombardment at the surface of the cathode. These electrons can be free after the impact under the high local electrical field (Fletcher, 1981).The study of these secondary emission effects is very important inside the cathode region.

From the previous studies, the electron current density produced by ion bombardment of the cathode with a γ coefficient, is determined by the following expression

$$j_e(0,t) = \gamma\ j_i(0,t) = \gamma\ n_i u_i \qquad 3.6.9$$

where j_e and j_i are the electron and ion current densities at the cathode respectively. Since experimental results on the dependence of the local field on the γ coefficient are not conclusive (Spyrou, 1996), the γ coefficient is generally assumed to be as 10^2.

In this study, simulation is done with and without these secondary emission effects. The study of the characteristics of the space charge is also carried out for both cases.

3.6.4 INITIAL SETTING OF THE SWARM PARAMETERS

Some coefficients such as the Townsend first ionization coefficient, α and recombination coefficient, β can be expressed as functions of the local reduced field E/p (Spyrou, 1996). This assumption implicitly mean that a local electric equilibrium is verified throughout the gap. Deviation from this state is produced when the field gradient is very sharp and the length of the formed sheath is smaller than the electron ionization mean free path. The above parameters are written as below

$$\frac{\alpha}{p} = 7.4326 \exp\left(-270.5\frac{p}{E}\right) \qquad \text{in } cm^{-1}Torr^{-1} \qquad 3.6.10$$

$$\beta = 6.3636 \times 10^{-12}\left(\frac{E}{p}\right)^{0.8} \qquad \text{in } cm^3 s^{-1} \qquad 3.6.11$$

The velocities of the electron and ion can also be expressed in the functions of the local reduced field E/p (in $Vcm^{-1}Torr^{-1}$) (Spyrou, 1991, 1996). There are

$$u_e = 2.9 \times 10^5\left(\frac{E}{p}\right) \qquad \text{in } cm\ s^{-1} \qquad 3.6.12$$

$$u_i = 1.67 \times 10^3\left(\frac{E}{p}\right) \qquad \text{in } cm\ s^{-1} \qquad 3.6.13$$

3.7 SATO'S EQUATION AS THE SOLUTION OF THE DISCHARGE CURRENT

From the formula derived in the last chapter, we can rewrite Eq(2.7.12), when a discharge is occurring in between two parallel plates. The equation can be presented as

$$I = \frac{eA}{d}\int_0^d (n_i u_i - n_e u_e)dx \qquad 3.7.1$$

where A is the discharge surface, d is the distance between the two electrodes.

Eq(3.7.1) can be easily solved numerically. The value of the discharge current is calculated and injected into the circuit equation to recalculate the dynamic resistance of the gap as shown in Eq(3.2.1b).

From this Sato's method, the discharge current was calculated based on the motion of the charged particles. This information is more reliable while comparing with the methods used for solving the circuit equation empirically, where the resistance of the discharge gap is assumed empirically (Iwasaki and Jitsuno, 1982; Papadopoulos, 1990; Dipace, 1987).

3.8 NUMERICAL ALGORITHM

In this section, the numerical algorithm of the new model will be discussed. Fig(3.8) shows a simple flow chart that summarizes the basic principle of the computational operation.

Before the simulation is began, assumptions of both the ion and electron densities in the discharge channel is needed. Both of these charge carriers are assumed uniformly distributed. The number density is assumed to be $1000cm^{-3}$ due to the cosmic radiation process. Some important parameters such as the mesh sizes for the space and time, Δx, and Δt have to be carefully selected to fulfill the requirement of the FCT algorithm for stability reasons. The details on these conditions have been discussed in the previous chapter.

As the first step of the simulation, RK-4 method is applied to solve the circuit equations. As a result, the voltage of the gap is first calculated. The gap voltage enables the determination of the local electrical field distribution by using the modified 1-D Poisson's equation. Some important parameters such as α, β, u_i and u_e can be calculated for every location in the channel. With these parameters, FCT will be used to solve the fluid equations and calculating the new density distribution for electron and ion at time $t + \Delta t$.

These new distributions will be used to calculate the internal discharge current and it will be calculated using Sato's equation. From here, the dynamic resistance of the discharge channel can be easily calculated with simple Ohm's law. This dynamic resistance will then be fed back into the circuit equation to complete the circle of the calculation.

These distributions of the charge carriers are also needed to simulate the local electrical field distribution for the next time step. Some useful data such as the discharge voltage, discharge current, time and space dependent electrical field and also the distribution of the charge carriers will be recorded.

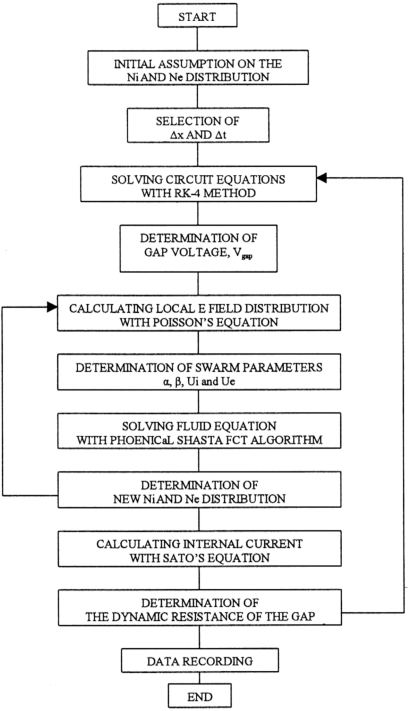

Figure 3.8: A Simple Chart Showing The Algorithm Of The Computer Model